# Statistical properties of the eigenvalue spectrum of the three-dimensional Anderson Hamiltonian

E. Hofstetter and M. Schreiber
*Institut für Physikalische Chemie, Johannes-Gutenberg-Universität, Jakob-Welder-Weg 11, D-55099 Mainz, Federal Republic of Germany*
(Received 25 May 1993)

A method to describe the metal-insulator transition (MIT) in disordered systems is presented. For this purpose the statistical properties of the eigenvalue spectrum of the Anderson Hamiltonian are considered. As the MIT corresponds to the transition between chaotic and nonchaotic behavior, it can be expected that the random matrix theory enables a qualitative description of the phase transition. We show that it is possible to determine the critical disorder in this way. In the thermodynamic limit the critical point behavior separates two different regimes: one for the metallic side and one for the insulating side.

It is now well established that the Anderson Hamiltonian, which is a widely used model to describe electronic states in disordered solids, exhibits a metal-insulator transition (MIT) in three-dimensional (3D) space. There are different ways[1] to show this but the usual way to determine this transition quantitatively is to calculate the decay length of the transmission probability using the transfer matrix method (TMM).[2] In this paper a quantitative method which is no longer based on the TMM but on the statistical properties of the energy spectrum will be presented.

The study of the energy spectrum has already provided very important results about the localization of the states[3,4] and about the kind of transport one can expect, e.g., superdiffusive, diffusive, or localized.[5–8] On the other hand, using the mathematical equivalence between the kicked rotator Hamiltonian and the Anderson Hamiltonian it was shown[8] that the MIT corresponds to a transition between a chaotic and a nonchaotic system. Here chaotic and nonchaotic mean, in the language of the random matrix theory (RMT),[9] that the fluctuations of the energy spectrum will obey the Gaussian orthogonal ensemble (GOE) and the Poisson ensemble (PE), respectively. Similar results were obtained[10,11] by studying the fluctuations of the number of levels in an energy band of given width for electrons moving in a random impurity potential. It has to be mentioned that recently Shklovskii *et al.*[12] have also considered the spacing distribution in order to study the MIT. Moreover, the study of the spectral fluctuations of the Lyapounov exponents in the framework of the TMM gave analogous results[13] and provided an explanation for the universal conductance fluctuations.[14]

The purpose of the present paper is to describe the transition from the metallic side that features the chaotic quantum spectrum to the insulating side where, due to the large disorder, the quantum interferences lead to the appearance of a nonchaotic quantum spectrum. The chaotic or nonchaotic behavior is given by the local properties of the spectrum, i.e., the fluctuations of levels around the average density of levels $\overline{\rho}(E)$. But if $\overline{\rho}(E)$ is not constant it will be impossible to compare the fluctuations in different parts of the spectrum in a straightforward way. In order to get rid of this problem one has to unfold the spectrum by means of the map[15] $E_i \rightarrow \varepsilon_i$ where

$$\varepsilon_i = \overline{N}(E_i) = N(E_i) - N_{\mathrm{fl}}(E_i). \tag{1}$$

Here $N(E_i)$ is the integrated density of levels and $N_{\mathrm{fl}}(E_i)$ denotes the fluctuations around the averaged integrated density of levels $\overline{N}(E_i)$.

For $s_i = \varepsilon_i - \varepsilon_{i-1}$ one can see easily that $\langle s_i \rangle = 1$ which means a constant density. Using the unfolded spectrum $\varepsilon_i$ the fluctuations can be appropriately characterized[9] by means of the spacing distribution $P(s)$ and the Dyson-Metha statistics $\Delta_3$. The first entity gives the distribution between consecutive levels and thus measures the level repulsion. $P(s)$ is normalized

$$\int P(s)\, ds = 1 \tag{2}$$

and it satisfies

$$\int P(s) s\, ds = 1 \tag{3}$$

due to definition (1). The second quantity $\Delta_3$ measures the deviation of a given sequence of levels from a perfectly uniform sequence, as a function of the average number of levels in the sequence. Thus it reflects the spectral rigidity. It is given by

$$\Delta_3(L) = \left\langle \frac{1}{L} \min_{A,B} \int_x^{x+L} [N(\varepsilon) - A\varepsilon - B]^2\, d\varepsilon \right\rangle_x , \tag{4}$$

where $\langle\,\rangle_x$ means that we average over different parts of the spectrum.

Using the RMT it is possible to calculate $P(s)$ and $\Delta_3$ for the two limiting cases of the spectrum, namely the GOE and the PE. For the metallic side one obtains[15]

 

$$P_{\mathrm{GOE}}(s) \simeq \frac{\pi}{2} s \exp\left(-\frac{\pi}{4} s^2\right), \tag{5}$$

$$\Delta_3(L) = \frac{2}{L^4} \int_0^L (L^3 - 2L^2 r + r^3) \Sigma^2(r)\, dr, \tag{6}$$

where $\Sigma^2(r)$ is the variance of the number of levels in a spectral window of width $r$. For the GOE it is given by

$$\Sigma^2(r) = \frac{2}{\pi^2}\left[\ln(2\pi r) + \gamma + 1 + \frac{1}{2}[\mathrm{Si}(\pi r)]^2 - \frac{\pi}{2}\mathrm{Si}(\pi r) - \cos(2\pi r) - \mathrm{Ci}(2\pi r) + \pi^2 r\left(1 - \frac{2}{\pi}\mathrm{Si}(2\pi r)\right)\right]. \tag{7}$$

The formula (5) for $P_{\mathrm{GOE}}(s)$ is exact only in the case of $2 \times 2$ matrices but remains a good approximation for the other cases. Important is the prefactor $s$ which shows the repulsion between the levels. For $\Delta_3$ there is no analytical solution and the integral (6) has to be calculated numerically.

For the localized case we have

$$P_{\mathrm{PE}}(s) = e^{-s}, \tag{8}$$

$$\Delta_3(L) = \frac{L}{15}. \tag{9}$$

In this case there is no longer any level repulsion but level clustering. As the localized states in different parts of the sample do not overlap and therefore cannot hybridize, their energy levels can become arbitrarily close.

The method described above will be applied now to the study of the Anderson model. The Hamiltonian is given by

$$H = \sum_i \epsilon_i |i\rangle\langle i| + \sum_{i \neq j} V |i\rangle\langle j|, \tag{10}$$

where it is generally assumed that the sites $i$ are distributed regularly in 3D space, e.g., on a simple cubic lattice. As usual we consider interactions only with the nearest neighbors and choose $V$=1 to define the energy scale. $\epsilon_i$ is the site energy and is described by a stochastic variable. In the present investigation we use a box distribution

$$p(\epsilon) = W^{-1}\theta(W/2 - |\epsilon|) \tag{11}$$

with variance $\sigma^2 = W^2/12$. $W$ represents the disorder and will be our critical parameter. It was shown previously[16] that the critical behavior at the MIT is independent of $p(\epsilon)$ at least for even distributions with well-defined momenta.

For very large disorder the diagonal element will be dominant and the spectrum will essentially be given by the random site energies which means that the fluctuations of the spectrum will obey the PE and the particle will be localized on one site. This reflects the fact that for large disorder the quantum interferences lead to the suppression of the diffusive processes. For very small disorder the interaction term will be dominant and will give rise to hybridization and thus to the repulsion between the energy levels. The particle will be delocalized. The problem is studying the transition between these two limiting regimes. For this purpose we calculated numerically the eigenvalues of the Anderson Hamiltonian. Due to the fact that we have interaction only with the nearest neighbors the Hamiltonian defines a very sparse secular matrix. Therefore we employ the Lanczos algorithm, which is suited to diagonalize such matrices. This was done for systems of size $M \times M \times M$ with $M$ ranging from 13 up to 21 and disorder $W$ from 2 to 40. We need to mention that the first attempt, to our knowledge, to describe numerically the evolution of the spacing distribution and the rigidity through the transition between the two regimes in a finite system was performed by Alt'shuler *et al.*[11] For $M = 5$ they obtained a Poissonian tail of $P(s)$ at the transition.

We are interested in the critical behavior at the band center ($E = 0$). But for the box distribution it was shown[17] that even far from the band center (up to $|E| = 5$) localized and extended states are separated by nearly the same critical disorder $W_c$ as for $E = 0$ and so are expected to be equivalent to the states at $E = 0$ as far as the determination of the critical behavior is concerned. In order to improve the accuracy of the calculation we will therefore consider a band of energy around $E = 0$ containing 50% of all levels, which corresponds to energies up to $|E| \simeq 1.8, 4.5, 10.2$ for $W = 2, 16.5, 40$, respectively. The calculation was performed for many different realizations of the disorder. The number of realizations was chosen so that $\sim 10^5$ eigenvalues were obtained for every pair of parameters $(M, W)$ which means between 25 and 90 realizations, for which the spectrum has been computed.

Using the set of eigenvalues $\{E_i\}$ obtained, we derive the average integrated density of levels $\overline{N}(E_i)$ in order to unfold our spectrum as already explained above. $\overline{N}(E_i)$ is determined by means of cubic spline interpolation as follows. A subset of the level spectrum consisting of points $[E_i, N(E_i)]$ with $i = 1, 101, 201, \ldots$ is chosen and the cubic splines through these points are applied in the interpolation. In this manner we get the unfolded spectrum $\{\varepsilon_i\}$. This allows us to study now the level fluctuation of our spectrum according to the spacing distribution $P(s)$ and the Dyson-Metha statistics $\Delta_3$. In order to quantify the change of the distribution as a function of the disorder and the size of the system we introduce a phenomenological formula for $P(s)$,[18]

$$P_{\mathrm{phe}}(s) = A s^{\beta}(1 + C\beta s)^{f(\beta)} \exp\left[-\frac{\pi^2}{16}\beta s^2 - \frac{\pi}{2}\left(1 - \frac{\beta}{2}\right) s\right] \tag{12}$$

with $f(\beta) = 2^{\beta}(1 - \beta/2)/\beta - 0.168\,74$, where $A$ and $C$ are normalization constants, so that Eqs. (2) and (3) are fulfilled.

This formula is an approximation for the extrapolation between our two limiting regimes GOE and PE. When

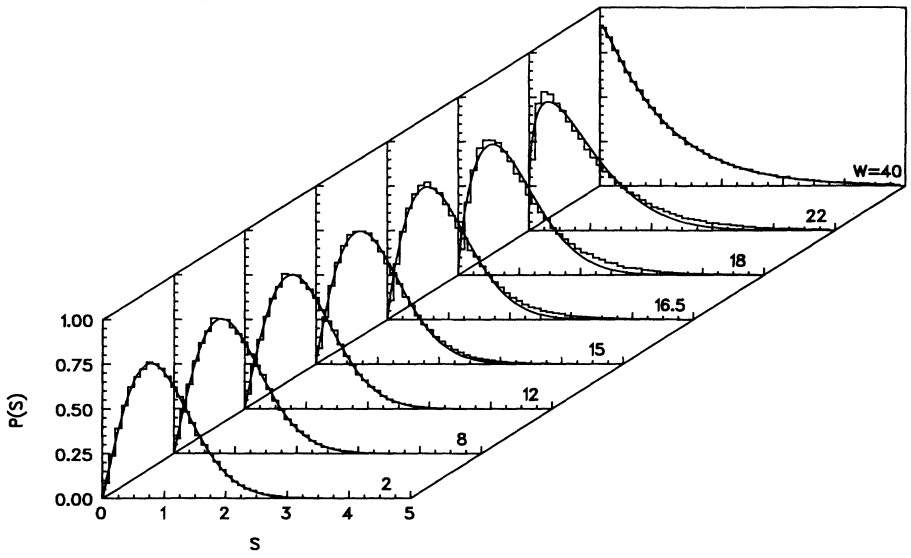


FIG. 1. Spacing distribution $P(s)$ for $M = 21$ and different disorders $W$. The histograms are the numerical results and the full lines are the fits according to the phenomenological formula (12). The distribution corresponds to the GOE for small $W$ and to the PE for large $W$.

$\beta = 1$ then $P_{\rm phe}(s) \simeq P_{\rm GOE}(s)$. It has to be noted that Eq. (12) gives a better approximation of the exact $P_{\rm GOE}(s)$ (Ref. 19) than the usual Wigner surmise distribution [Eq. (5)], which is exact only for $2 \times 2$ matrices as mentioned. For $\beta \to 0$ one has to perform an expansion of $As^{\beta}(1 + C\beta s)^{f(\beta)}$ to see that $P_{\rm phe}(s) \to P_{\rm PE}(s)$.

In Fig. 1 we have plotted $P(s)$ for $M = 21$ and different disorders. The histograms are the numerical results and the full lines show the fit for $P_{\rm phe}(s)$ with $s \in [0; 5]$. For small disorder the fluctuations are described, as expected, by the GOE and for large disorder by the PE. We can nicely see the transition from one regime to the other as a function of the disorder. The phenomenological formula gives a good description for $P(s)$ although in the intermediate regime we can see some discrepancy between the numerical results and $P_{\rm phe}(s)$ for $s > 2$. In order to take this into account $P(s)$ was fitted, for the subsequent calculation of $\beta$, $A$, and $C$, by $P_{\rm phe}(s)$ with $s \in [0.1; 2.0]$. The results are shown in Fig. 2 for $\beta(M, W)$. For $W$ from 2 to 15 we observe $\beta(M, W) \simeq 1$ independent of the size of the system. Then it begins to decrease and finally reaches $\beta(M, W) = 0$ for large disorder. It has to be noted that when $M$ is larger $\beta(M, W)$ decreases more slowly for $14 < W < 17$, but faster for $W > 17$. So in the thermodynamic limit we expect a step function for $\beta(\infty, W)$. This means $\beta = 1$ for $W < 17$ and $\beta = 0$ for $W > 17$. The value $W \simeq 17$ is the critical disorder $W_c$. The rough estimation of $W_c$ is in good agreement with previous results obtained within the framework of the TMM.[20] The value $\beta(M, W_c)$ is a fixed point, i.e., independent of $M$. This implies that for $M \to \infty$ we will have three different distributions for $P(s)$: one for $W < W_c$, one for $W = W_c$, and one for $W > W_c$. Similar results have been found by Shklovskii *et al.*[12] for $P(s)$.

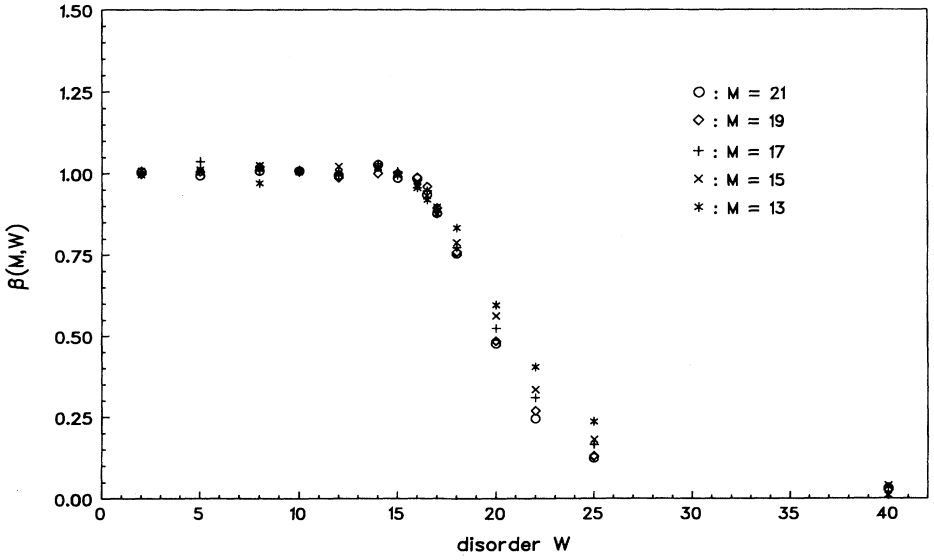


FIG. 2. Values of the fitted parameter $\beta(M, W)$. $\beta = 1$ corresponds to the GOE case and $\beta = 0$ to the PE case.

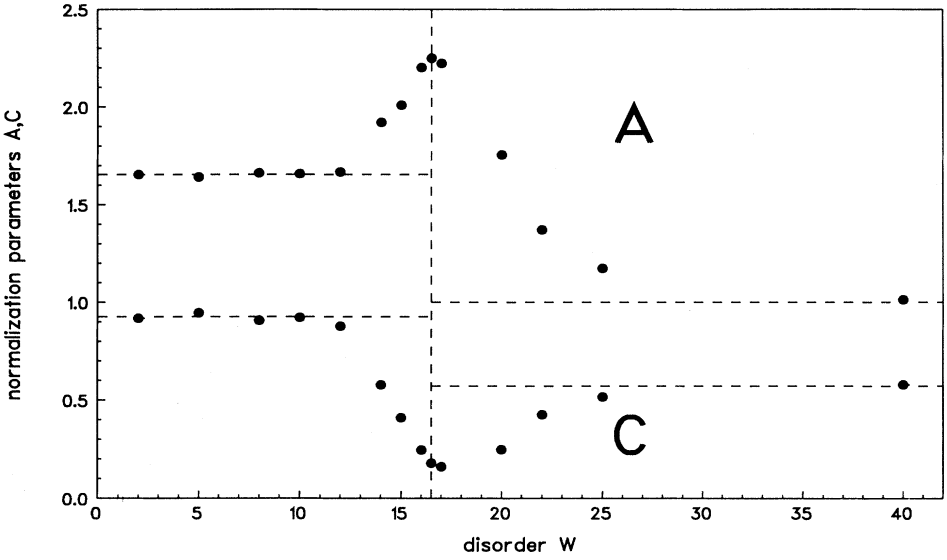


FIG. 3. Values of the normalization parameters $A$ and $C$ for $M = 21$ and different disorders $W$. The vertical dashed line is the expected value of $W_c = 16.5$. On the left-hand side of this separating line the horizontal dashed lines represent the values of $A$ and $C$ for the GOE and on the right-hand side the respective values for the PE.

They showed that this intermediate distribution between GOE and PE features the small-$s$ behavior of the first ensemble and the large-$s$ behavior of the second ensemble, respectively, in contrast, for the large-$s$ behavior, with our results.

In Fig. 3 the values of the normalization parameters $A$ and $C$ for $M = 21$ are given. The vertical dashed line is the expected value of $W_c = 16.5$.[20] On the left-hand side of this separating line the horizontal dashed lines represent the values of $A$ and $C$ for the GOE. These values are numerically computed using the results of Dietz and Haake.[19] On the right-hand side the dashed lines reflect the respective values for the PE which can be calculated analytically. We see that the normalization constants give very interesting information about the phase transition in particular for the critical disorder $W_c$. The accuracy of $C$ is not as good as that of $A$ due to numerical problems during the fit but even so $C$ remains an indicator for the critical disorder.

We enlarge the transition regime of Fig. 3 to study the behavior of $A$ in more detail in Fig. 4. We observe that the values of $A$ decrease from the value at the critical disorder to the two limiting values of $A$. Except at the critical disorder and (due to numerical inaccuracies also) in the close vicinity of $W_c$ this decrease becomes faster when $M$ increases. This indicates that in the thermodynamic limit we will have only three different values of $A$ and so three different distributions of $P(s)$ as already mentioned above. Analogous results are obtained from the analysis of $C$.

In Fig. 5 we report the results obtained for the Dyson-Metha statistics. Again we clearly see the transition between the chaotic and the nonchaotic regime as a function of the disorder $W$. If we now investigate what happens as

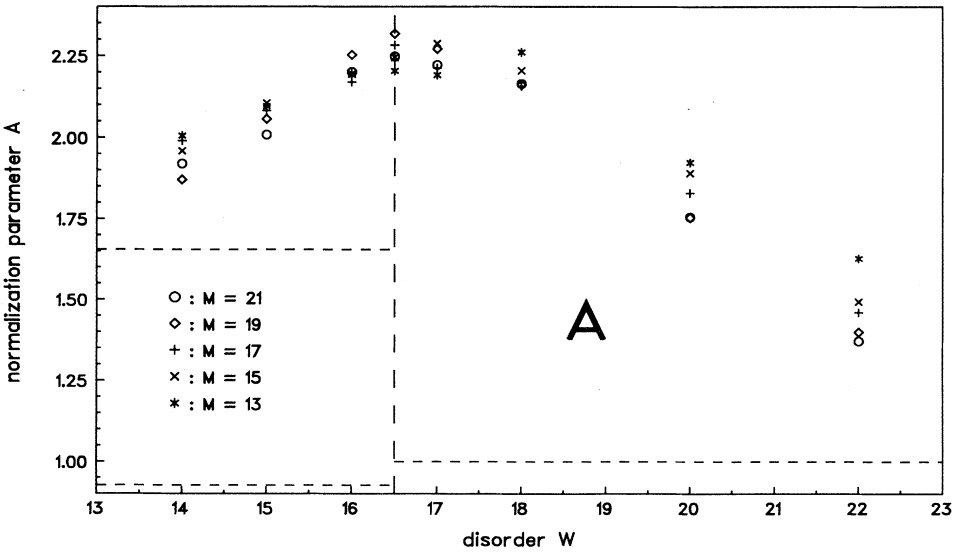


FIG. 4. Details of Fig. 3 for the normalization parameter $A$ in the vicinity of the critical disorder $W_c$ for different system sizes.

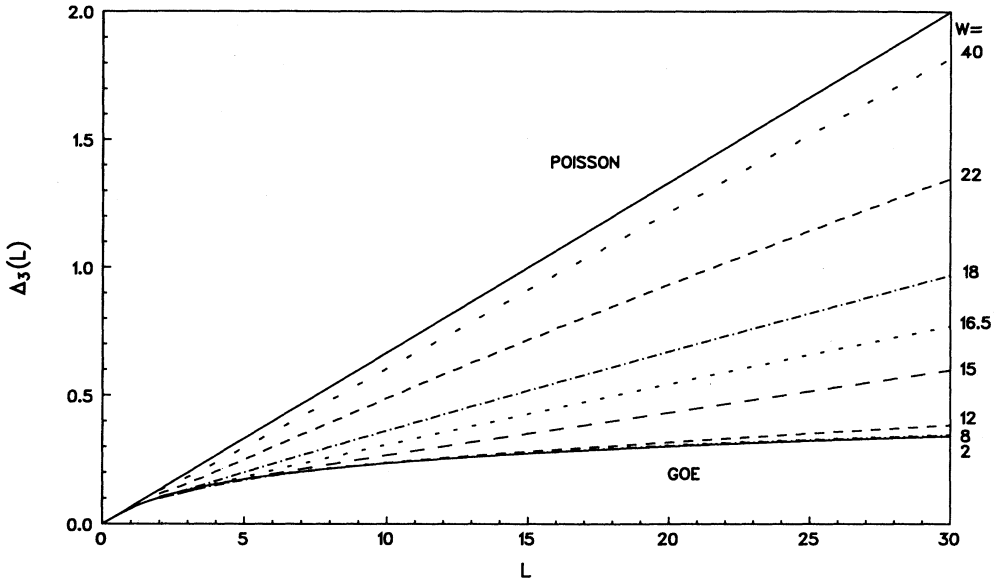


FIG. 5. Dyson-Metha statistics $\Delta_3(L)$ for $M = 21$. The transition from GOE to Poisson statistics occurs as a function of the disorder $W$ (denoted on the right-hand side).

a function of the system size $M$ for $W = 14, 16.5$, and 20 we observe in Fig. 6 that for $W < W_c$ the $\Delta_3$ curve moves in the direction towards the GOE case when $M$ increases. For $W > W_c$ we have the opposite behavior, this time the curve moves in the direction of the PE case. Finally for $W = W_c$ we have the same curve independent of the system size. This reflects the three different regimes expected in the thermodynamic limit as already seen for $P(s)$.

Another interesting point to consider is the shape of $\Delta_3(L)$ for $W < W_c$ which is presented in more detail in Fig. 7. We see that for every $W$ a critical value $L_c$ can be defined up to which $\Delta_3(L)$ coincides with the GOE case. As already seen, for larger $L$ the $\Delta_3$ – curves move away in the direction of the $W_c$ case. For $W \to W_c$ we observe $L_c \to 0$. The meaning of $L_c$ can be directly related to the Thouless energy $E_c$ (Ref. 21) in the following way. It was shown[10] that for an energy bandwidth $E < E_c$ the fluctuation in the number of levels is described by the GOE case. For $E > E_c$ the fluctuations are larger than expected for the GOE. This can be seen by the calculation of

$$\Sigma^2(E) = \langle N(E)^2 \rangle - \langle N(E) \rangle^2, \tag{13}$$

where $\Sigma^2$ is the variance of the number of energy levels in a spectral window of width $E$ as in Eq. (7) except that in Eq. (7) we consider the rescaled energy of the unfolded spectrum instead of the energy. The Thouless energy $E_c$ can be explained in the following way. In a chaotic system the particle can diffuse in the whole system and so it can reach the edges of the sample. Because of this the particle will be very sensitive to any change

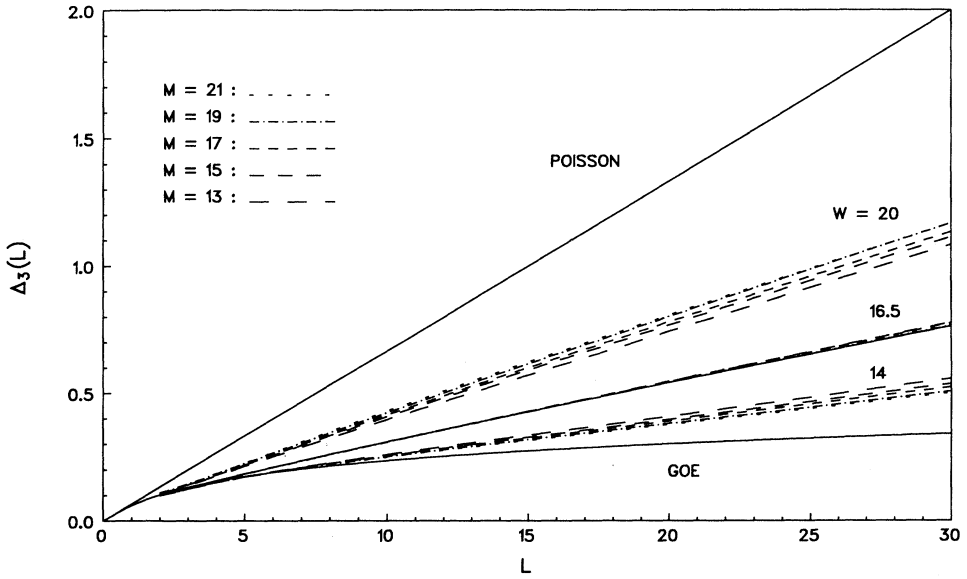


FIG. 6. Dyson-Metha statistics $\Delta_3(L)$ for various system sizes $M$ and $W = 14, 16.5$, and 20. With increasing $M$ the $\Delta_3$ curve moves towards the GOE limit for $W < W_c$ and towards the Poisson limit for $W > W_c$. For $W = W_c$ the curve is independent of the system size.

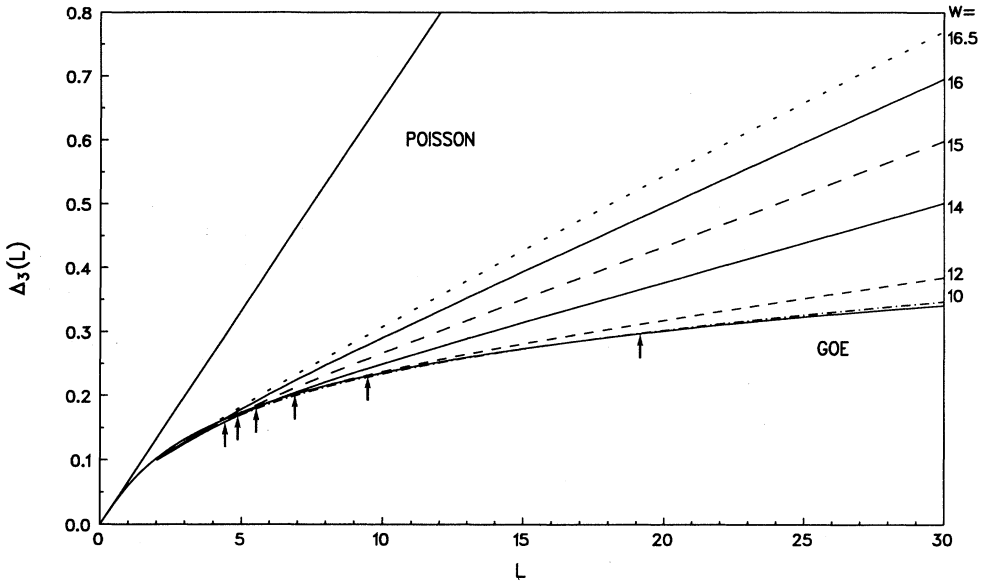


FIG. 7. Dyson-Metha statistics $\Delta_3(L)$ for $M = 21$ and different disorders $W < W_c$. A critical value $L_c$ can be defined (see arrows) up to which $\Delta_3(L)$ is given by the GOE curve.

of the boundary conditions and $E_c$ very large. On the other hand in the nonchaotic system the diffusion is suppressed so that the particle is no longer sensitive to any change of the boundary conditions and thus $E_c \to 0$. If we now consider a sequence of energy levels, then the length of the sequence $L$ corresponds to the energy bandwidth $E$, and the above discussed critical value $L_c$ corresponds to the Thouless energy $E_c$. There is, however, an important difference, because $L$ refers to the unfolded spectrum. Therefore we expect the same $L_c$ to be valid for the whole spectrum except for the large energy tails in which the states are localized even for small $W$. Another way to determine the MIT, by scaling theory, for the rigidity, was suggested by Alt'shuler *et al.*,[11] claiming that $\Sigma^2(E) = \alpha\langle N(E)\rangle$ with $\alpha \simeq 0.25$ at the transition point. This result has, however, not been confirmed by their numerical work,[11] nor by our present analysis of the unfolded spectrum for considerably larger systems.

Finally we would like to come back briefly to the spacing distribution $P(s)$. In Fig. 8 we have plotted $P(s)$ for $M = 21$ and various disorders, $2 \leq W \leq 40$. For $s \simeq 2$ all the curves have the same value, and further investigations have shown that this point is also independent of $M$. A possible explanation is the following. If it would be possible to scale $P(s)$ with respect to the system size we would expect two points independent of the size and of the disorder, namely $s = 0$ and $s = \infty$, one curve $P(s)$ for $W = W_c$ independent of the size, and all the other curves size dependent. The above discussed behavior of the thermodynamic limit of $P(s)$ as well as its properties at $W_c$ suggest that some finite-size scaling behavior may be possible. This would require the possibility of defining

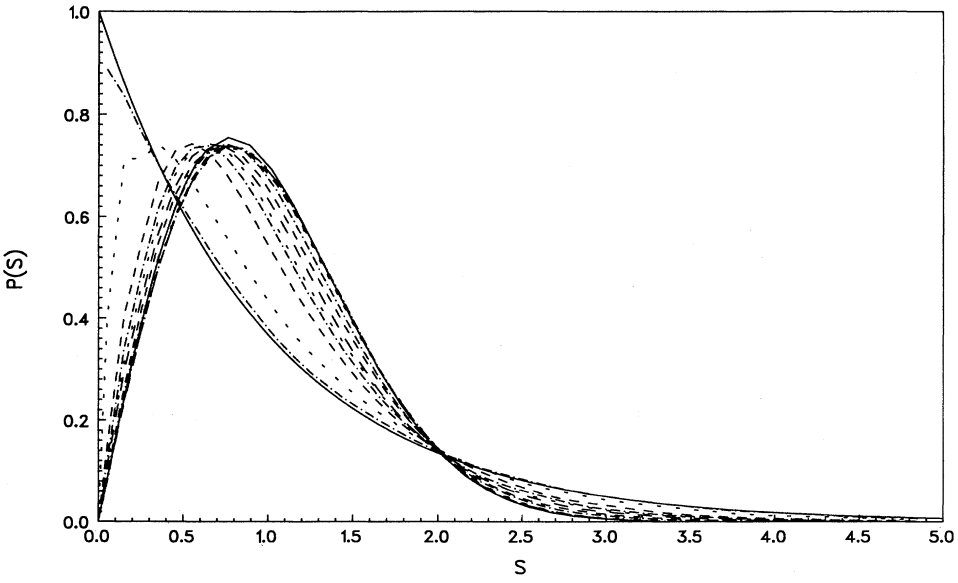


FIG. 8. Spacing distribution $P(s)$ for $M = 21$ and $W = 0$, 2, 5, 8, 10, 12, 14, 15, 16, 16.5, 17, 18, 20, 22, 40, $\infty$ (from top to bottom at $s = 1.2$). The fixed point for $s_0 \simeq 2$ is independent of the system size.

a characteristic quantity $\alpha$ which can be expressed by a scaling function $f$ as $\alpha(M,W) = f[M/\xi_\infty(W)]$, where $\xi_\infty(W)$ is the correlation length for an infinite system. A possible choice for $\alpha$ would be to calculate the area between $P(s)$ and the $s$ axis for $s \in [0,\infty]$. But one has to remember that $P(s)$ is normalized according to Eq. (2) so that we will obtain a constant for the respective integral. In order to find the supposed finite-size scaling behavior we "need" a new boundary except $s = 0$ and $s = \infty$ for the integration. This is naturally provided by the appearance of the fixed point $s_0 \simeq 2$. Now two possible regions can be considered, namely from 0 to $s_0$ and from $s_0$ to $\infty$. Preliminary investigations show that the supposed finite-size scaling is indeed possible. Respective results will be published elsewhere.

In conclusion the study of the statistical properties of the energy spectrum gives a suitable method to describe the MIT. The calculation of the spacing distribution $P(s)$ and the spectral rigidity $\Delta_3(L)$ yields three different regimes for finite systems. For $W < W_c$ and $W > W_c$, the results depend on the system size $M$ and tend towards the GOE, and to the PE, respectively, when $M$ increases. For $W = W_c$ the results are independent of the system size. This gives a criterion to determine the critical disorder $W_c$. The estimation of $W_c$ is in good agreement with previous calculations[20] using the TMM. Another consequence of this behavior is that in the thermodynamic limit three different regimes of the system are expected, for $W < W_c$ the GOE regime, for $W = W_c$ an intermediate case between GOE and PE, and finally for $W > W_c$ the PE regime. We would like to mention in this context that although three different regimes have been found only two of them, namely the GOE and the PE, have a physical meaning. The intermediate case is defined only for one peculiar value of the disorder, the critical disorder, and thus cannot be measured because the point $W_c$ will never be reached with an absolute accuracy. For infinite systems we will always be in the GOE or in the PE regimes. The intermediate case can be considered as a marginal case without physical significance.

It will be interesting to include 100% of the levels into the present investigation. Until now it was very difficult to study the critical behavior in the band edge of the spectrum so the comparison between the here presented case in which 50% of the levels around the band center were considered and the 100% case could provide some information about this problem. It should be realized, however, that localized and extended states would be included in such an analysis simultaneously which might render the investigation even more complicated.

The size-dependent behavior of the results with the fixed point at $W_c$ suggests some finite-size scaling behavior and the possibility defining characteristic quantities, based on $P(s)$ or $\Delta_3$, described by a finite-size scaling function. This supposition is supported by the results for $P(s)$ in Fig. 8. The computation of this finite-size scaling function should allow a better determination of the critical disorder $W_c$ as well as the calculation of the critical exponents for the MIT without needing the correlation length for a finite system as in the TMM. The rough estimates of these critical values obtained by Shklovskii *et al.*[12] are in agreement with our results.[22]


[1] E. N. Economou, C. M. Soukoulis, and A. D. Zdetsis, Phys. Rev. B **30**, 1686 (1984); F. Wegner, in *Localization, Interaction and Transport Phenomena*, edited by B. Kramer, G. Bergmann, and Y. Bruynseraede, Springer Series in Solid State Sciences Vol. 61 (Springer-Verlag, Berlin, 1985), p. 99; D. Vollhardt and P. Wölfle, Phys. Rev. B **22**, 4666 (1980); Phys. Rev. Lett. **48**, 699 (1982); S. Sarker and E. Domany, Phys. Rev. B **23**, 6081 (1981).

[2] A. MacKinnon and B. Kramer, Phys. Rev. Lett. **47**, 1546 (1981); Z. Phys. B **53**, 1 (1983).

[3] H. Kunz and B. Souillard, Commun. Math. Phys. **78**, 201 (1980).

[4] J. Fröhlich and T. Spencer, Commun. Math. Phys. **88**, 151 (1983).

[5] D. H. Dunlap, H.-L. Wu, and P. W. Philips, Phys. Rev. Lett. **65**, 88 (1990).

[6] B. Simon, Adv. Appl. Math. **3**, 463 (1982).

[7] J. Kollar and A. Süto, Phys. Lett. A **117**, 203 (1986).

[8] D. R. Grempel, R. E. Prange, and S. Fishman, Phys. Rev. A **29**, 1639 (1984).

[9] *Statistical Theories of Spectra: Fluctuations*, edited by C. E. Porter (Academic, New York, 1965); M. L. Metha, *Random Matrices* (Academic, New York, 1991).

[10] B. L. Alt'shuler and B. I. Shklovskii, Zh. Eksp. Teor. Fiz. **91**, 220 (1986) [Sov. Phys. JETP **64**, 127 (1986)].

[11] B. L. Alt'shuler, L. Kh. Zharekeshev, S. A. Kotochigova, and B. I. Shklovskii, Zh. Eksp. Teor. Fiz. **94**, 343 (1988) [Sov. Phys. JETP **67**, 625 (1988)].

[12] B. I. Shklovskii, B. Shapiro, B. R. Sears, P. Lambrianides, and H. B. Shore, Phys. Rev. B **47**, 11 487 (1993).

[13] J.-L. Pichard, N. Zanon, Y. Imry, and A. D. Stone, J. Phys. France **51**, 587 (1991).

[14] Y. Imry, Europhys. Lett. **1**, 249 (1986).

[15] O. Bohigias and J.-M. Giannoni, in *Mathematical and Computational Methods in Nuclear Physics*, edited by J. Dehesa, J. Gomez, and A. Polls, Lecture Notes in Physics Vol. 209 (Springer, Berlin, 1984), p. 1; O. Bohigias, J.-M. Giannoni and C. Schmit, Phys. Rev. Lett. **52**, 1 (1984).

[16] E. Hofstetter and M. Schreiber, Europhys. Lett. **27**, 933 (1993).

[17] B. Bulka, M. Schreiber, and B. Kramer, Z. Phys. B **66**, 21 (1987).

[18] G. Casati, F. Izrailev, and L. Molinari, J. Phys. A **24**, 4755 (1991).

[19] B. Dietz and F. Haake, Z. Phys. B **80**, 153 (1990).

[20] B. Kramer, K. Broderix, A. MacKinnon, and M. Schreiber, Physica A **167**, 163 (1990).

[21] D. J. Thouless, Phys. Rev. Lett. **39**, 1167 (1977).

[22] E. Hofstetter and M. Schreiber (unpublished).